Electronic Supplementary Information (ESI)

Two heterovalent copper–organic frameworks with multiple secondary building units: high performance of gas adsorption and separation, I_2 sorption and release

Shuo Yao,[a] Xiaodong Sun,[a] Bing Liu,[a] Rajamani Krishna,[b] Guanghua Li,[a] Qisheng Huo,[a] and Yunling Liu*[a]

a. State Key Laboratory of Inorganic Synthesis and Preparative Chemistry, College of Chemistry, Jilin University, Changchun 130012, P. R. China

**E-mail: yunling@jlu.edu.cn; Fax: +86-431-85168624; Tel: +86-431-85168614*

b. Van't Hoff Institute for Molecular Sciences, University of Amsterdam, Science Park 904, 1098 XH Amsterdam, The Netherlands. E-mail: r.krishna@contact.uva.cl.

S1. Calculation procedures of selectivity from IAST

The measured experimental data is excess loadings (q^{ex}) of the pure components CO_2, CH_4, C_2H_6 and C_3H_8 for **JLU-Liu31**, which should be converted to absolute loadings (q) firstly.

$$q = q^{ex} + \frac{pV_{pore}}{ZRT}$$

Here Z is the compressibility factor. The Peng-Robinson equation was used to estimate the value of compressibility factor to obtain the absolute loading, while the measure pore volume 0.85 $cm^3\ g^{-1}$ is also necessary.

The dual-site Langmuir-Freundlich equation is used for fitting the isotherm data at 298K.

$$q = q_{m_1} \times \frac{b_1 \times p^{1/n_1}}{1 + b_1 \times p^{1/n_1}} + q_{m_2} \times \frac{b_2 \times p^{1/n_2}}{1 + b_2 \times p^{1/n_2}}$$

Here p is the pressure of the bulk gas at equilibrium with the adsorbed phase (kPa), q is the adsorbed amount per mass of adsorbent (mol kg^{-1}), q_{m1} and q_{m2} are the saturation capacities of sites 1 and 2 (mol kg^{-1}), b_1 and b_2 are the affinity coefficients of sites 1 and 2 (1/kPa), n_1 and n_2 are the deviations from an ideal homogeneous surface.

The selectivity of preferential adsorption of component 1 over component 2 in a mixture containing 1 and 2, perhaps in the presence of other components too, can be formally defined as

$$S = \frac{q_1/q_2}{p_1/p_2}$$

q_1 and q_2 are the absolute component loadings of the adsorbed phase in the mixture. These component loadings are also termed the uptake capacities. We calculate the values of q_1 and q_2 using

the Ideal Adsorbed Solution Theory (IAST) of Myers and Prausnitz.

S2. Calculations of the isosteric heats of gas adsorption (Q_{st})

A virial-type expression comprising the temperature-independent parameters a_i and b_j was employed to calculate the enthalpies of adsorption for CH_4, C_2H_6 and C_3H_8 (at 273 and 298 K) on compounds. In each case, the data were fitted using the equation:

$$ln^P = ln^N + {}^1/_T \sum_{i-0}^{m} a_i N^i + \sum_{j-0}^{n} b_j N^j$$

Here, P is the pressure expressed in Torr, N is the amount adsorbed in mmol g^{-1}, T is the temperature in K, a_i and b_j are virial coefficients, m, n represent the number of coefficients required to adequately describe the isotherms (m and n were gradually increased until the contribution of extra added a and b coefficients was deemed to be statistically insignificant towards the overall fit, and the average value of the squared deviations from the experimental values was minimized). The values of the virial coefficients a_0 through a_m were then used to calculate the isosteric heat of adsorption using the following expression.

$$Q_{st} = -R \sum_{i-0}^{m} a_i N^i$$

Q_{st} is the coverage-dependent isosteric heat of adsorption and R is the universal gas constant. The heats of gas sorption for JLU-Liu31 in this manuscript are determined by using the sorption data measured in the pressure range from 0-1 bar (273 and 298 K for gases), which is fitted by the virial-equation very well.

S3. Supporting Figures

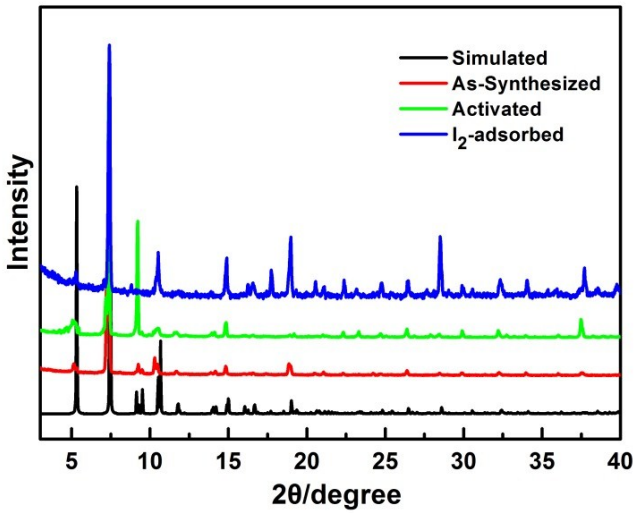

Fig. S1 PXRD patterns of JLU-Liu31 for simulated, as-synthesized, activated and I_2-adsorbed samples. The differences in reflection intensity are probably due to preferred orientations in the powder samples.

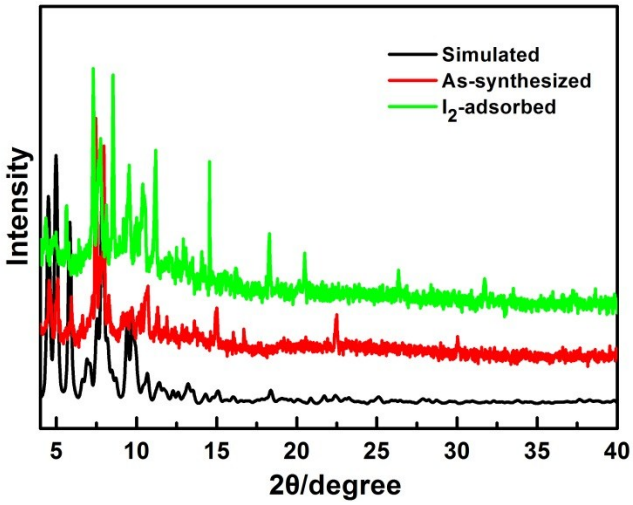

Fig. S2 PXRD patterns of JLU-Liu32 for simulated, as-synthesized and I_2-adsorbed samples. The differences in reflection intensity are probably due to preferred orientations in the powder samples.

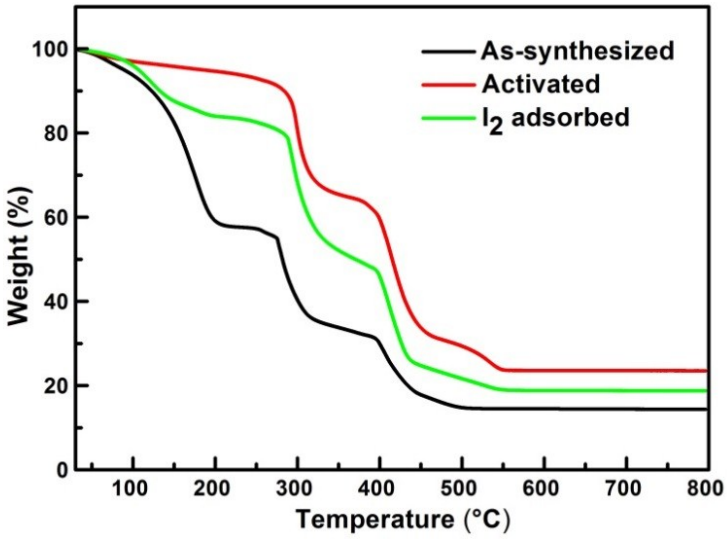

Fig. S3 TGA curves of JLU-Liu31 for the as-synthesized, activated and iodine adsorbed samples.

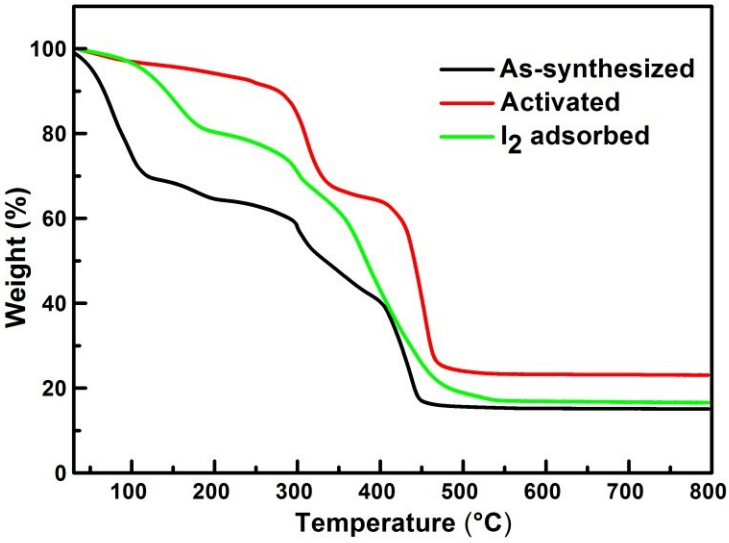

Fig. S4 TGA curves of JLU-Liu32 for the as-synthesized, activated and iodine adsorbed samples.

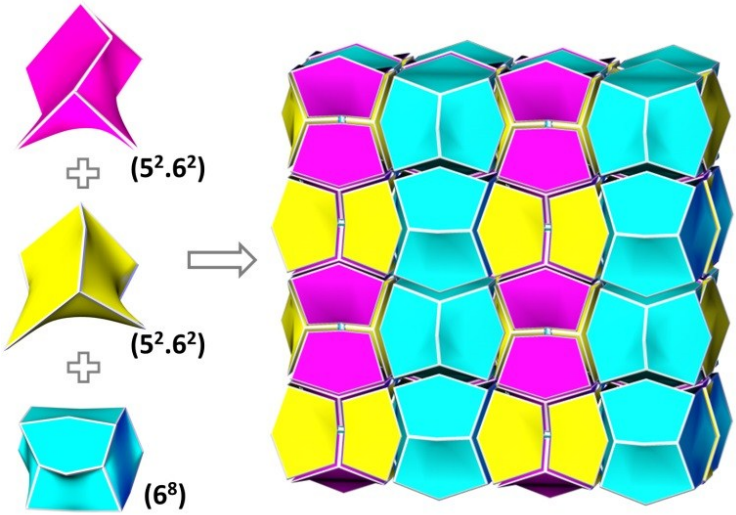

Fig. S5 Topological features of JLU-Liu31 displayed by tiles and face symbols for pink, yellow and blue tiles are $(5^2.6^2)$, $(5^2.6^2)$ and (6^8).

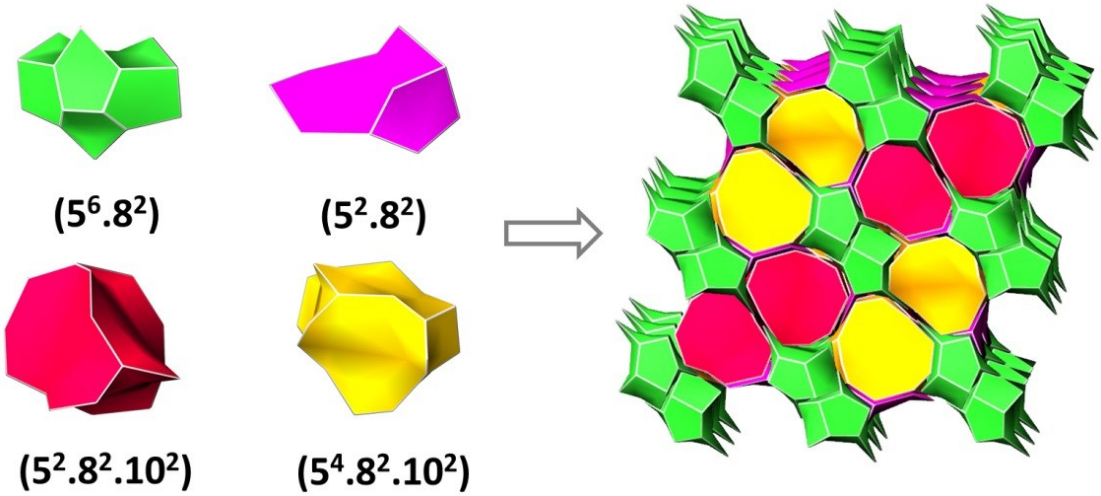

Fig. S6 Topological features of JLU-Liu32 displayed by tiles and face symbols for green, pink, red and yellow tiles are $(5^6.8^2)$, $(5^2.8^2)$, $(5^2.8^2.10^2)$ and $(5^4.8^2.10^2)$.

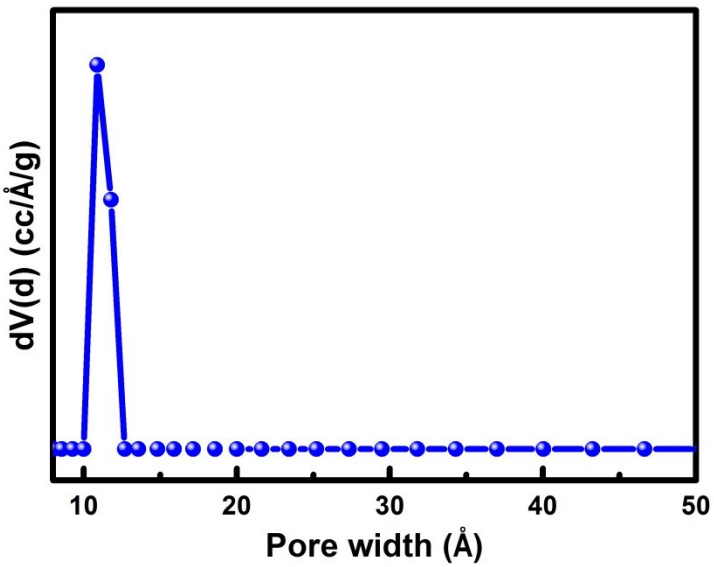

Fig. S7 The pore size distribution of JLU-Liu31 calculated by using the DFT method.

In order to ensure the accuracy and repeatability of results for the gas adsorption and isosteric heats of JLU-Liu31, we prepare another three batches of samples to make parallel experiments and get another three sets of data for H_2, CO_2, CH_4, C_2H_6 and C_3H_8. Fig. S8-12 shows the three sets of adsorption isotherms for the five kinds of gases and their isosteric heats calculated by viral method.

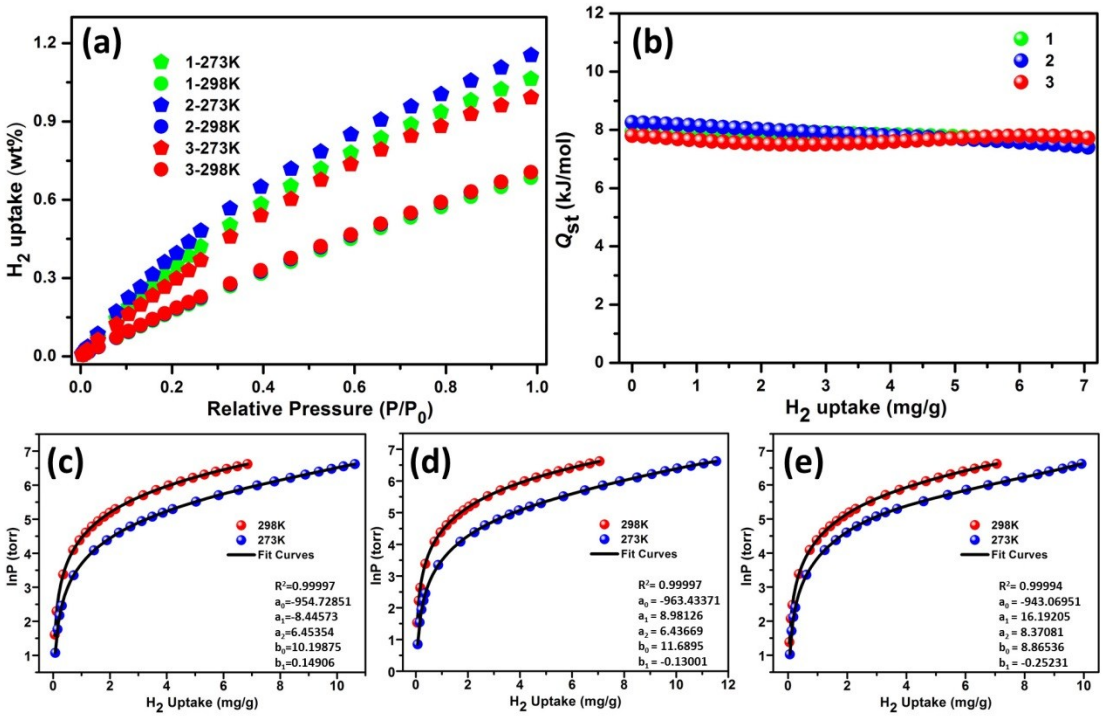

Fig. S8 (a) H_2 sorption isotherms of JLU-Liu31 for three batches of samples at 77 and 87 K; (b) isosteric heats of H_2 for the corresponding three samples; (c)-(e) nonlinear curves fitting of H_2 for the corresponding three samples.

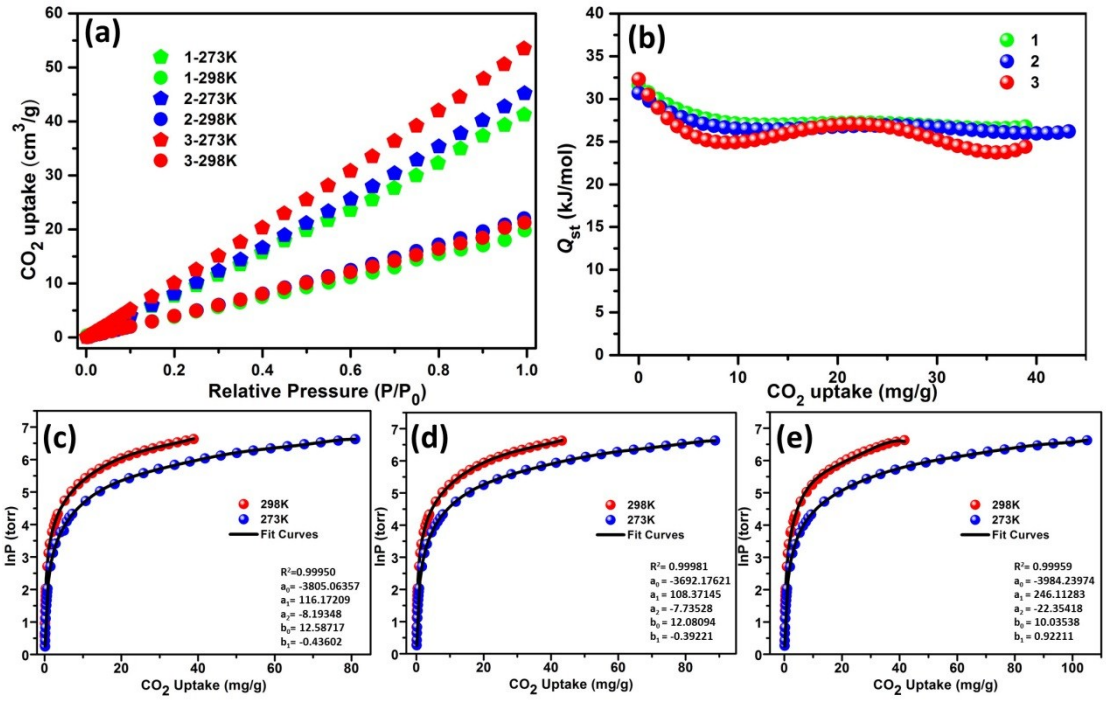

Fig. S9 (a) CO_2 sorption isotherms of JLU-Liu31 for three batches of samples at 273 and 298 K; (b) isosteric heats of CO_2 for the corresponding three samples; (c)-(e) nonlinear curves fitting of CO_2 for the corresponding three samples.

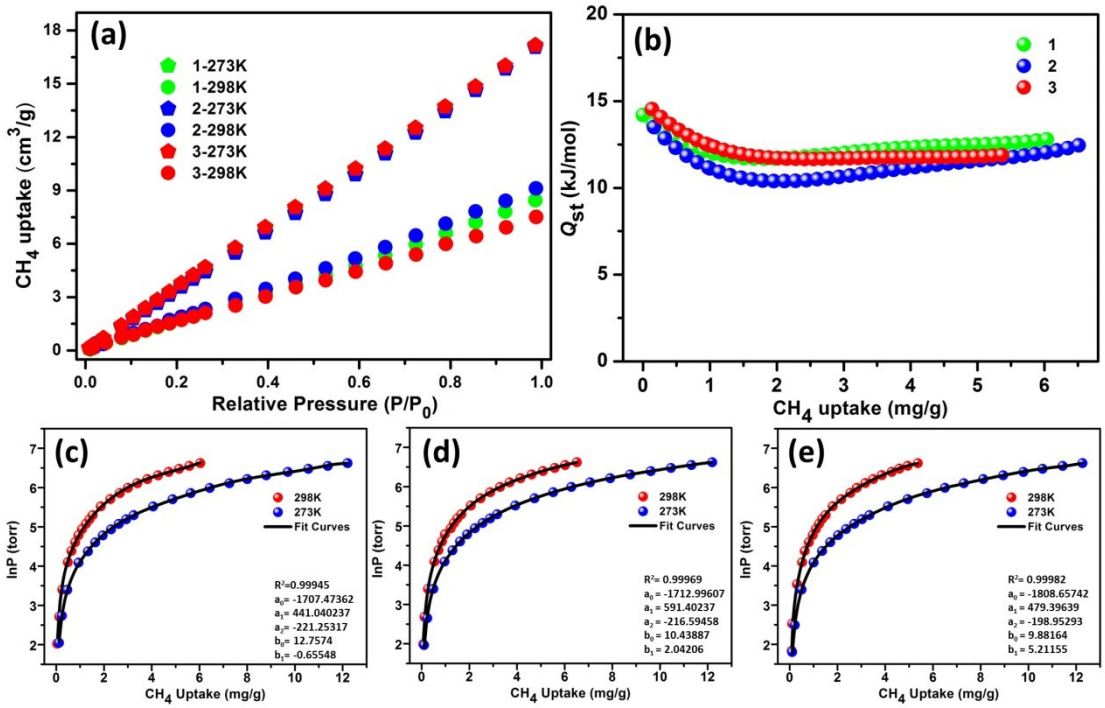

Fig. S10 (a) CH_4 sorption isotherms of JLU-Liu31 for three batches of samples at 273 and 298 K; (b) isosteric heats of CH_4 for the corresponding three samples; (c)-(e) nonlinear curves fitting of CH_4 for the corresponding three samples.

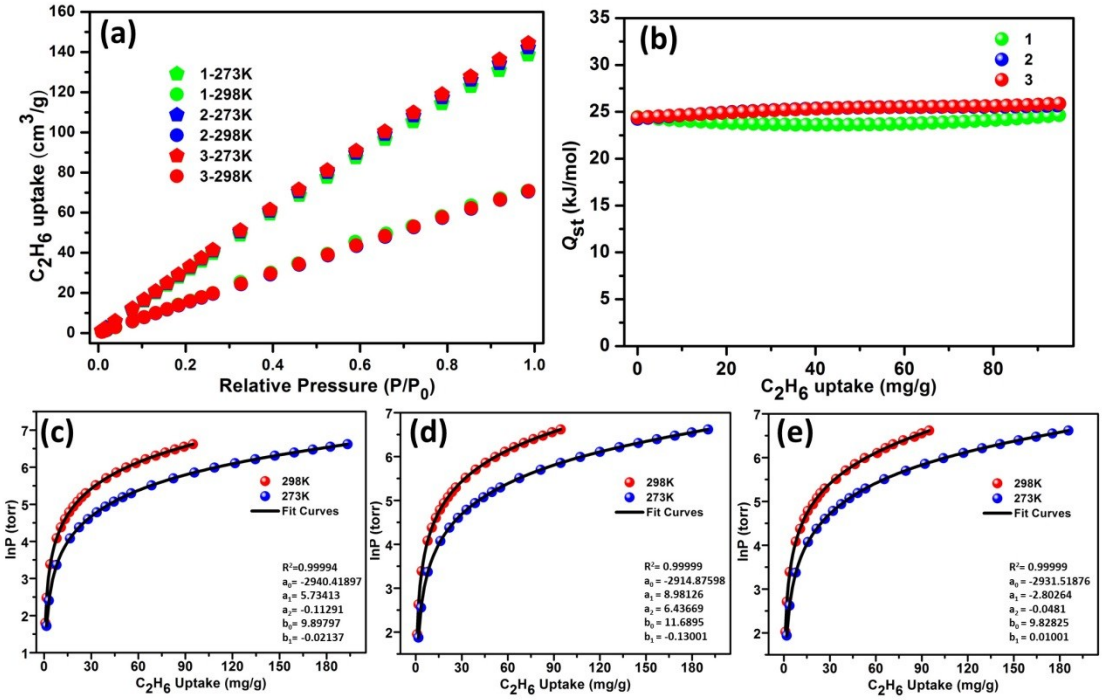

Fig. S11 (a) C_2H_6 sorption isotherms of JLU-Liu31 for three batches of samples at 273 and 298 K; (b) isosteric heats of C_2H_6 for the corresponding three samples; (c)-(e) nonlinear curves fitting of C_2H_6 for the corresponding three samples.

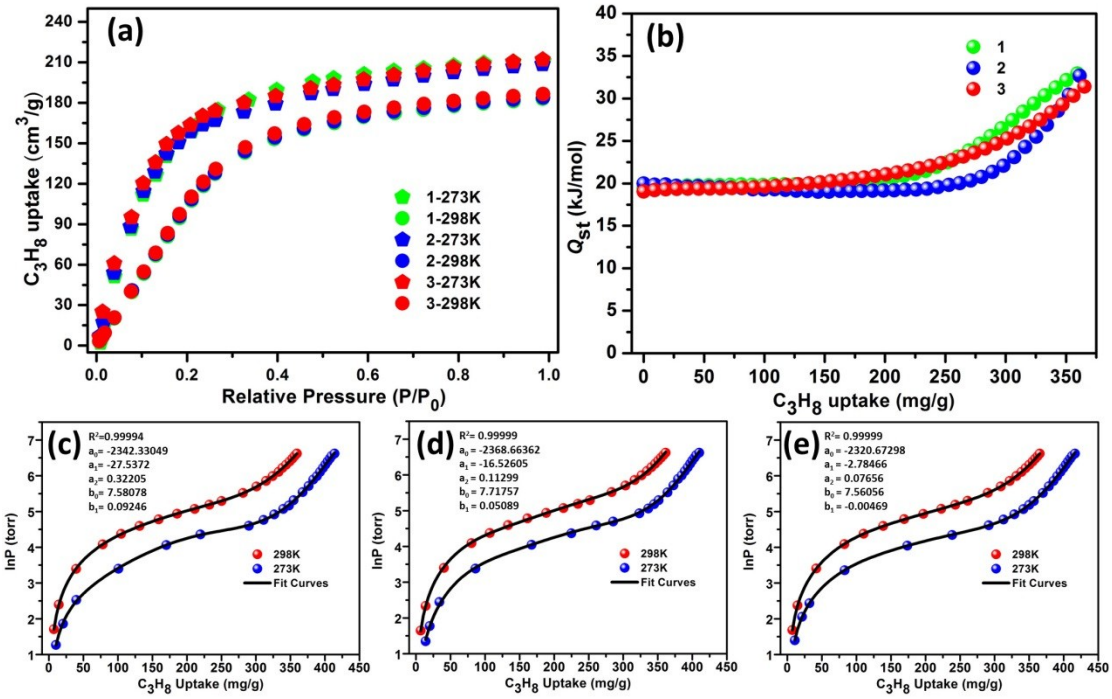

Fig. S12 (a) C_3H_8 sorption isotherms of JLU-Liu31 for three batches of samples at 273 and 298 K; (b) isosteric heats of C_3H_8 for the corresponding three samples; (c)-(e) nonlinear curves fitting of C_3H_8 for the corresponding three samples.

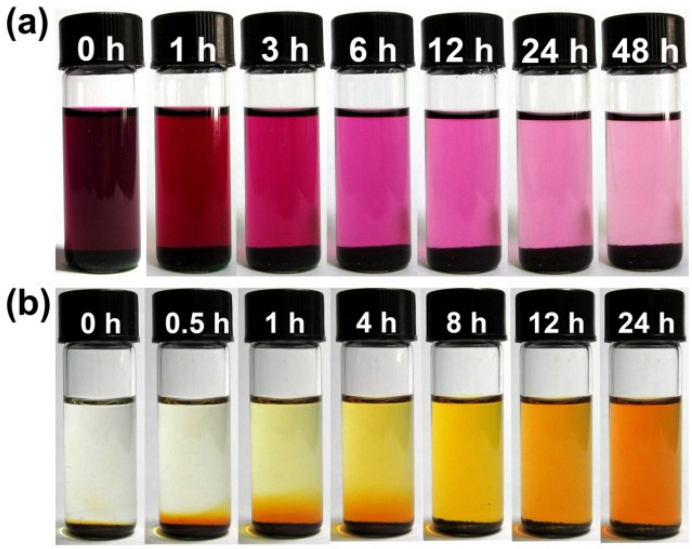

Fig. S13 (a) Photographs of time-dependent I_2 adsorption process of 100 mg JLU-Liu31 in 3mL cyclohexane. (b) Photographs of time-dependent I_2 release process of 20 mg JLU-Liu31 in 3 mL ethanol.

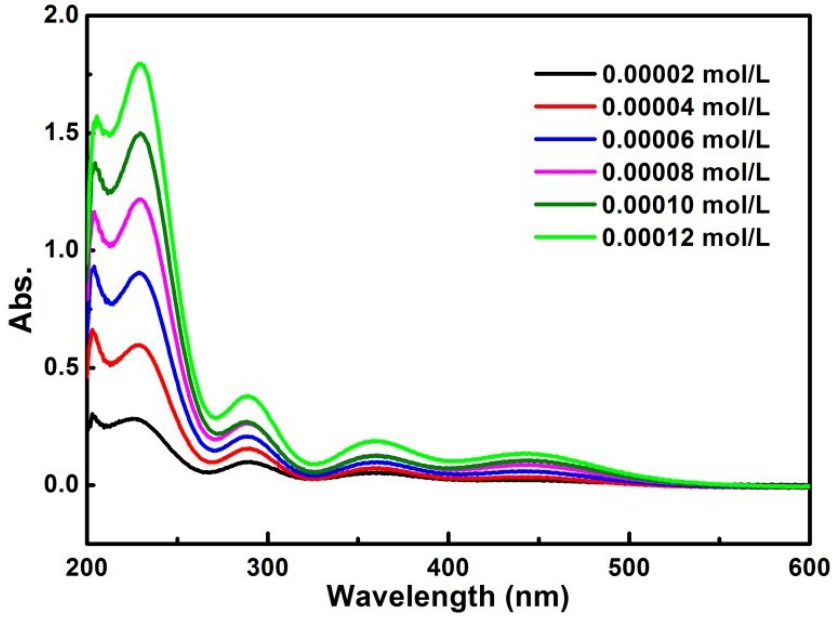

Fig. S14 UV-vis spectra of iodine in ethanol.

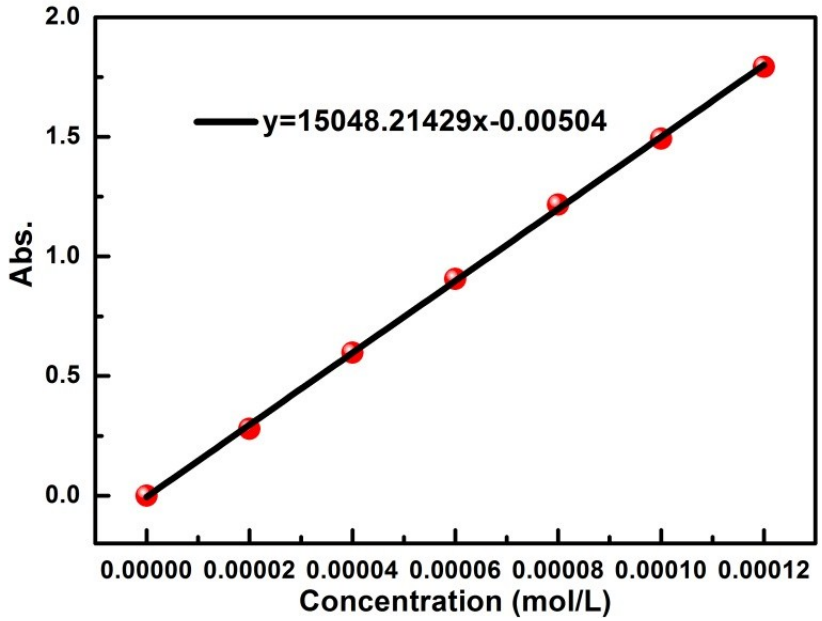

Fig. S15 Calibration plot of standard iodine by UV-vis spectra.

S4. Supporting Tables

Table S1. Crystal data and structure refinements for JLU-Liu31 and JLU-Liu32

compound	**JLU-Liu31**	**JLU-Liu32**
Formula	$C_{136}H_{180}Cu_8I_4N_{24}O_{32}$	C_{123} H_{185} Cu_7 I_4 $N_{27}O_{32}$
Formula weight	3678.95	3506.36
Temperature (K)	293(2)	296(2)
Wavelength (Å)	0.71073	0.71073
Crystal system	orthorhombic	orthorhombic
Space group	*Cmcm*	*Pnnm*
a (Å)	33.712(7)	34.9115(8)
b (Å)	19.058(4)	41.3131(9)
c (Å)	33.611(7)	28.9710(6)
α (°)	90	90
β (°)	90	90
γ (°)	90	90
V (Å^3)	21595(7)	41784.9(16)
Z, D_c (Mg/m^3)	4,1.132	8, 1.116
F(000)	7456	14280
θ range (deg)	1.208-25.326	2.24-19.44
reflns collected/unique	68324/10118	272669/37874
R_{int}	0.0846	0.1228
data/restraints/params	10118/0/277	37874/77/878
GOF on F^2	1.034	0.836
R_1, wR_2 (I>2σ(I))	0.0492, 0.1465	0.0499, 0.1173
R_1, wR_2 (all data)	0.0750, 0.1575	0.1302, 0.1332

Since the highly disordered guest molecules were trapped in the channels of the two compounds and could not be modeled properly, there are "Alert level A" about "Check Reported Molecular Weight" and "VERY LARGE Solvent Accessible VOID(S) in Structure" in the "checkCIF/PLATON report" files for JLU-Liu31 and JLU-Liu32. The final formula of JLU-Liu31 and JLU-Liu32 were derived from crystallographic data combined with elemental and thermogravimetric analysis data.

Table S2. The topological information for JLU-Liu31 and JLU-Liu32 calculated by TOPOS 4.0 and Systre.

Compound JLU-Liu31

Vertex figure										
Vertex	CS1	CS2	CS3	CS4	CS5	CS6	CS7	CS8	CS9	CS10
V1	3	13	29	61	98	148	199	268	334	428
V2	3	13	29	59	99	143	201	268	337	421
V3	6	18	38	66	108	156	212	272	354	430
V4	4	8	28	62	104	140	218	266	352	408
Vertex	**Extended point symbols**									
V1	[5.5.6(3)]									
V2	[5.5.6(3)]									
V3	[5.5.5.5.6.6.6.6.6.6.6.6.8(4).9(2).9(2)]									
V4	[5.5.5.5.6(2).6(2)]									

Compound JLU-Liu32

Vertex figure										
Vertex	CS1	CS2	CS3	CS4	CS5	CS6	CS7	CS8	CS9	CS10
V1	3	10	20	42	57	92	135	185	220	282
V2	3	10	20	41	63	102	117	179	223	297
V3	3	11	21	37	57	99	137	178	224	265
V4	5	13	26	36	74	109	151	175	229	297
V5	4	8	24	44	70	80	134	154	256	288
V6	4	8	24	34	56	84	133	179	219	264
V7	6	16	24	40	70	122	154	188	222	292
V8	4	9	20	39	70	86	134	183	231	274
Vertex	**Extended point symbols**									
V1	[5.5.8(3)]									
V2	[5.5.8(3)]									
V3	[5.5.5]									
V4	[5.5.5.5.5.8(2).8(2).8(3).8.8]									
V5	[5.5.8.8.11(8).11(8)]									
V6	[5.5.5.8(3).8.8]									
V7	[5.5.5.5.5.5.5.8(3).8(3).8(3).8(3).8(2).8(2).8(4)]									
V8	[5.5.5.8(2).5.8(2)]									

Table S3. The adsorption amounts of JLU-Liu31 for H_2, CO_2, CH_4, C_2H_6 and C_3H_8 for four batches of samples.

	BET (m^2 g^{-1})	H_2 (wt%)		CO_2 (cm^3 g^{-1})		CH_4 (cm^3 g^{-1})		C_2H_6 (cm^3 g^{-1})		C_3H_8 (cm^3 g^{-1})	
		77K	87K	273K	298K	273K	298K	273K	298K	273K	298K
1	1700	1.17	0.54	35	17	14	8	142	68	191	169
2	1690	1.06	0.68	41	20	17	8	138	70	210	182
3	1610	1.15	0.70	45	22	17	9	142	70	208	183
4	1640	0.99	0.70	53	21	17	7	144	70	212	186

Table S4. The H_2, CO_2, CH_4, C_2H_6 and C_3H_8 isosteric heats of JLU-Liu31 for four batches of samples.

`	H_2 (kJ/mol)	CO_2 (kJ/mol)	CH_4 (kJ/mol)	C_2H_6 (kJ/mol)	C_3H_8 (kJ/mol)
1	16.8	32.6	13	25	20
2	7.9	31.6	14	25	19
3	8.0	30.7	11	24	20
4	7.8	32.3	12	24	19

Table S5. The refined parameters for the Dual-site Langmuir-Freundlich equations fit for the pure isotherms of CO_2, CH_4, C_2H_6 and C_3H_8 for JLU-Liu31 at 298 K.

	q_{m1}	b_1	n_1	q_{m2}	b_2	n_2	R^2
CO_2	83.78106	0.18044	0.00163	9.71841E-5	1.01298	11.14388	0.99998
CH_4	0.10733	2.50388	7.60184E-10	0.00148	4.58951	0.97001	0.99994
C_2H_6	4.43346	0.01554	0.00688	6.52596E-5	1.00354	1.67025	0.99999
C_3H_8	2.30909	5.99418	1.45516E-5	0.03516	3.79119	1.13518	0.99999